Table II, it is clear that the calculated $B(E2)$ values are quite good, and at the worst are off by a factor of $\frac{1}{2}$. This is certainly encouraging. The enhancement ratio of the calculated $B(E2)$ to the single-particle estimate varies in the range 2–15. The agreement between the calculated and the experimental half-lives of the states is quite fair. From the calculated intensity ratio of $E2$ to $M1$ transitions, the transitions from the first excited state to the ground state are almost pure $M1$ type in all odd-A nuclei studied.

Though we are keeping V_0 and α fixed for all the nuclei, the effect of the variation of these parameters on the quadrupole and magnetic moment has been studied in case of two nuclei ^{23}Na and ^{25}Mg. This is shown in Fig. 1. It is seen that the magnitudes of Q as well as μ increase with increasing V_0 and decrease with increasing α. However, the variation is slow and quite smooth.

IV. CONCLUSION

A formulation to calculate the electromagnetic properties of nuclei, the form factors in electron scattering, ft values in β decay, and the reduced widths of nuclear states in the direct reaction has been developed, in order to test the nuclear wave functions obtained from a determinantal HF state by the projection technique. Employing a phenomenological internucleon interaction in the form of a Rosenfeld mixture with Yukawa radial dependence, we have calculated the quadrupole and magnetic moments, $B(E2)$ values, and half-lives of nuclear states in a number of nuclei in the sd shell. In view of the fact that we have kept all the parameters fixed, the agreement obtained between the experimental and calculated values over the whole region of the sd-shell nuclei is quite good. It should also be mentioned at this stage that the excited spectra, the binding energies,[5] and the electromagnetic properties of a large number of nuclei in a region are successfully explained by treating all the particles in the system. We also plan to calculate the other nuclear properties described in this paper.

It should, however, be mentioned that since we started from a determinantal HF state for neutrons and protons together, in certain cases it may happen that our projected wave functions do not have a good isospin quantum number. We believe that because of the variational nature of the HF state, the admixture of the excited isospin state would be quite small. It may also be mentioned that our restriction in the HF calculations to orbitals in the sd shell may not be a good approximation for when the total number of nucleons is large. We plan to investigate these points in the near future.

PHYSICAL REVIEW VOLUME 159, NUMBER 4 20 JULY 1967

Energy Levels and Electromagnetic Transitions in N^{15} from the $C^{13}(He^3,p\gamma)N^{15}$ Reaction*

G. W. PHILLIPS,† F. C. YOUNG, AND J. B. MARION
University of Maryland, College Park, Maryland

(Received 13 March 1967)

Excited states of N^{15} have been studied by the $C^{13}(He^3,p\gamma)N^{15}$ reaction. Proton spectra were measured with a magnetic spectrometer at two angles for He^3 energies of 2 and 5 MeV. Excitation energies of 9.054±0.004, 9.225±0.003, 9.829±0.004, and 10.072±0.004 MeV were obtained for levels in N^{15}. Electromagnetic branching ratios were measured for levels at 8.31, 8.57, 9.05, 9.16, 9.22, 9.76, 9.83, 9.93, 10.07, and 10.45 MeV. A comparison was made with theoretical branching ratios calculated from shell-model wave functions for levels at 8.31, 8.57, 9.05, and 9.93 MeV. Measured branching ratios for the first three of these levels agree with calculated ratios for shell-model levels of $J^\pi=\frac{1}{2}^+$, $\frac{3}{2}^+$, and $\frac{1}{2}^+$, respectively. Proton–γ-ray angular-correlation measurements for levels at 9.05, 9.16, and 9.22 MeV indicate $J=\frac{3}{2}$ for the 9.16-MeV state, $J=\frac{1}{2}$ or $\frac{3}{2}$ for the 9.05-MeV level, and $J=\frac{3}{2}$ (90% probability) or $J=\frac{1}{2}$ (10% probability) for the 9.22-MeV level.

I. INTRODUCTION

THE mirror nuclei, N^{15} and O^{15}, are of considerable theoretical interest because in the shell model their lowest-order configurations have only a single hole within the closed $(1s)^4(1p)^{12}$ shell. Thus, shell-model calculations for the low-lying levels are relatively straightforward and are expected to agree reasonably well with experiment. Apart from the Z projection of the isobaric-spin quantum number, the theoretical treatment of N^{15} and O^{15} is identical (neglecting Coulomb-energy effects). Where spins and parities are known, it should be possible to identify experimental levels in N^{15} with their isobaric analog levels in O^{15} which have theoretical wave functions that differ only in T_z.

* Research supported in part by the U. S. Atomic Energy Commission.

† Present address: University of Washington, Seattle, Washington.

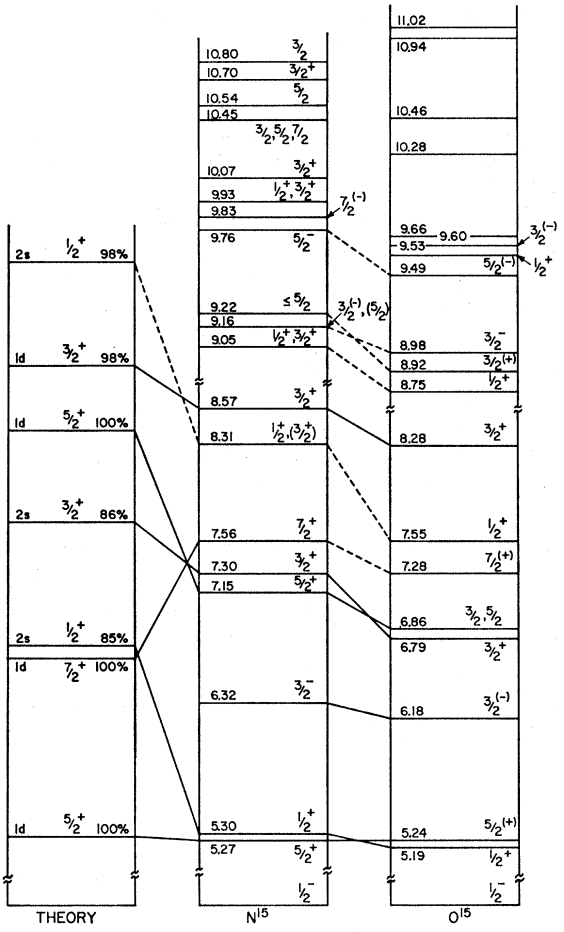

FIG. 1. Experimental energy levels in N^{15} and O^{15} and theoretical even-parity levels for mass 15.

Energy levels for mass 15 were included in a shell-model study of light nuclei by Inglis.[1] Kurath[2] has performed individual-particle-model calculations for the normal-parity levels of $1p$ shell nuclei. For $A=15$, two levels result with spins and parities of $\frac{1}{2}^-$ and $\frac{3}{2}^-$, which in N^{15} correspond to the ground state and the level observed at 6.32 MeV, respectively. Halbert and French[3,4] have obtained individual-particle-model wave functions for even-parity levels of mass-15 nuclei, which can be identified reasonably well with the experimental levels in N^{15} up to 9 MeV. Above 9 MeV, theoretical work has been hampered, not only by the greater complexity of the shell-model configurations which become possible at higher energies,[3,5] but also by the previous lack of detailed experimental data concerning the bound states in N^{15} above 9 MeV. Figure 1 shows the experimental energy levels[6–10] of N^{15} and O^{15} and the first seven theoretical even-parity levels of Halbert and French.[3,4]

Previous direct experimental observations of the energy levels in N^{15} consist primarily of magnetic-spectrograph and electrostatic-deflection measurements from the $N^{14}(d,p)N^{15}$ and $C^{13}(He^3,p)N^{15}$ reactions.[11–14] At the time this work was undertaken the structure of the bound levels in N^{15} above 8-MeV excitation was not well understood. Clarification of the level structure in this energy region and precise excitation energies have been provided by the recent work of Gallman *et al.*[14] Independent accurate determinations of the excitation energies of the levels in N^{15} up to 10.07 MeV were reported[9] while this work was in progress. The energies of the levels at 9.76 and 9.93 MeV can be accurately determined from the threshold energies in the $C^{14}(d,n)N^{15}$ reaction,[9,15] and the unbound levels at 10.45 MeV and above have been observed directly as resonances in the $C^{14}(p,\gamma)N^{15}$ reaction.[16–18] The present magnetic-spectrometer measurements provide additional precise excitation energies for the states at 9.05, 9.22, 9.83, and 10.07 MeV.

Information on spins and parities of the levels in N^{15} comes from $N^{14}(d,p)N^{15}$ stripping results,[19–21] γ-ray angular-correlation measurements,[9,22–25] and internal pair-production correlation measurements.[9] By these methods, spins and parities have been established for the levels up to 8 MeV.[9] Recent proton–γ-ray angular-

[1] D. R. Inglis, Rev. Mod. Phys. **25**, 390 (1953).
[2] D. Kurath, Phys. Rev. **101**, 216 (1956).
[3] E. C. Halbert, Ph.D. thesis, University of Rochester, 1956 (unpublished).
[4] E. C. Halbert and J. B. French, Phys. Rev. **105**, 1563 (1957).
[5] E. C. Halbert (private communication).
[6] T. Lauritsen and F. Ajzenberg-Selove, Nucl. Phys. **11**, 1 (1959).
[7] T. Lauritsen and F. Ajzenberg-Selove, in *Nuclear Data Sheets*, compiled by K. Way, *et al.* (Printing and Publishing Office, National Academy of Sciences—National Research Council, Washington, D. C., 1962), sets 5 and 6.
[8] A. E. Evans, B. Brown, and J. B. Marion, Phys. Rev. **149**, 863 (1966).
[9] E. K. Warburton, J. W. Olness, and D. E. Alburger, Phys. Rev. **140**, B1202 (1965).
[10] A. E. Evans, Phys. Rev. **155**, 1047 (1967).
[11] A. Sperduto, W. W. Buechner, C. K. Bockelman, and C. P. Browne, Phys. Rev. **96**, 1316 (1954).
[12] R. A. Douglas, J. W. Broer, Ren Chiba, D. F. Herring, and E. A. Silverstein, Phys. Rev. **104**, 1059 (1956).
[13] T. E. Young, G. C. Phillips, R. R. Spencer, and D. A. A. S. N. Rao, Phys. Rev. **116**, 962 (1959).
[14] A. Gallmann, P. Fintz, J. B. Nelson, and D. E. Alburger, Phys. Rev. **147**, 753 (1966).
[15] R. Chiba, Phys. Rev. **123**, 1316 (1961).
[16] G. A. Bartholomew, F. Brown, H. E. Gove, A. E. Litherland, and E. B. Paul, Can. J. Phys. **33**, 441 (1955).
[17] D. F. Hebbard and D. N. E. Dunbar, Phys. Rev. **115**, 624 (1959).
[18] D. F. Hebbard, Nucl. Phys. **19**, 551 (1960).
[19] R. D. Sharp, A. Sperduto, and W. W. Buechner, Phys. Rev. **99**, 632 (1955).
[20] T. S. Green and R. Middleton, Proc. Phys. Soc. (London) **A69**, 28 (1955).
[21] E. K. Warburton and J. N. McGruer, Phys. Rev. **105**, 639 (1957).
[22] S. Gorodetzky, P. Fintz, G. Bassompierre, and A. Gallman, Compt. Rend. **252**, 713 (1961).
[23] G. A. Bartholomew and J. F. Vervier, Nucl. Phys. **50**, 209 (1964).
[24] E. K. Warburton, J. S. Lopes, R. W. Ollerhead, A. R. Poletti, and M. F. Thomas, Phys. Rev. **138**, B104 (1965).
[25] D. Pelte, B. Povh, and W. Scholz, Nucl. Phys. **78**, 241 (1966).

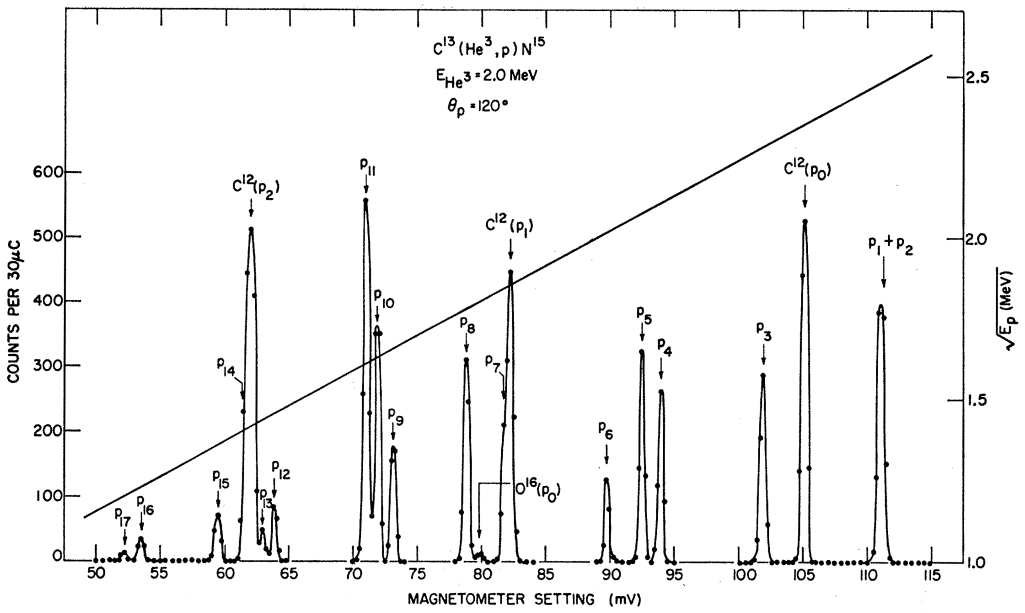

FIG. 2. Proton momentum profile for the $C^{13}(He^3,p)N^{15}$ reaction at an incident beam energy of 2 MeV and a magnetic-spectrometer angle of 120°. Proton groups from O^{16} and C^{12} in the target are labeled by the target nucleus.

correlation measurements have also given values for the spins of the levels at 8.57, 9.76, 9.83, and 10.07 MeV.[26]

γ-ray branching ratios have been reported previously[9,25–28] for excited states of N^{15} and are fairly complete up to about 9 MeV. These are useful in substantiating spin and parity assignments and for comparison with theory. Above 9 MeV, most previous investigations have been hampered by the difficulty in resolving the triplet of levels at 9.05, 9.16, and 9.22 MeV and the quadruplet of levels at 9.76, 9.83, 9.93, and 10.07 MeV. For the majority of these levels only the strongest γ-ray branches have been observed.[9]

In the present work, detailed branching ratios were obtained for the levels from 8.31 to 10.45 MeV in N^{15} by measuring γ-ray spectra with a large NaI(Tl) crystal in coincidence with proton groups resolved with the magnetic spectrometer. In this way it was possible to observe branches as small as 1% and to set upper limits of about 1% for most unobserved branches involving a γ ray of energy greater than about 1 MeV. Theoretical electromagnetic transition rates for the levels at 8.31, 8.57, 9.05, and 9.93 MeV were calculated for comparison with the experimental branching ratios. In addition, proton–γ-ray angular-correlation measurements were made for the levels at 9.05, 9.16, and 9.22 MeV in N^{15} to determine the spins of these levels. A preliminary report of this work has been given.[29]

II. ENERGY LEVELS AND BRANCHING RATIOS IN N^{15}

A. Procedure

The target chamber and detector geometry used for the γ-ray branching ratio measurements have been described previously.[30,31] A cylindrical target chamber was used with a 5-in.-diam×5-in. NaI(Tl) γ-ray detector placed above the target with its face $\frac{3}{4}$ in. from the target center. To minimize absorption of the γ rays, the top of the chamber was made of Al machined to a thickness of 0.050 in. Particles from the reaction were analyzed by a 180° double-focusing magnetic spectrometer and detected by a solid-state detector at the exit of the magnet. The spectrometer was connected to the chamber by a sliding seal which allowed it to rotate from 0° to 125° with respect to the incident beam direction about an axis coincident with the axis of the NaI(Tl) detector. Targets were thin, self-supporting carbon foils[31,32] made by cracking methyl iodide (CH_3I)[33] enriched to about 60% in C^{13}.

The path of particles through the spectrometer bends

[26] E. K. Warburton and J. W. Olness, Phys. Rev. **147**, 698 (1966).
[27] H. T. Motz, R. E. Carter, and W. D. Barfield, in *Pile Neutron Research in Physics* (International Atomic Energy Agency, Vienna, 1962), p. 225.
[28] R. E. Carter and H. T. Motz, in *International Conference on Nuclear Physics with Pile Reactor Neutrons*, edited by F. E. Throw (Argonne National Laboratory, Argonne, Illinois, 1963), p. 179.
[29] G. W. Phillips, F. C. Young, and J. B. Marion, Bull. Am. Phys. Soc. **11**, 27 (1966).
[30] F. C. Young, H. T. Heaton, G. W. Phillips, P. D. Forsyth, and J. B. Marion, Nucl. Instr. Methods **44**, 109 (1966).
[31] V. A. Latorre, Ph.D. thesis, University of Maryland, 1965 (unpublished).
[32] W. R. Harris (private communication).
[33] Obtained from Isomet Corporation, Palisades Park, New Jersey.

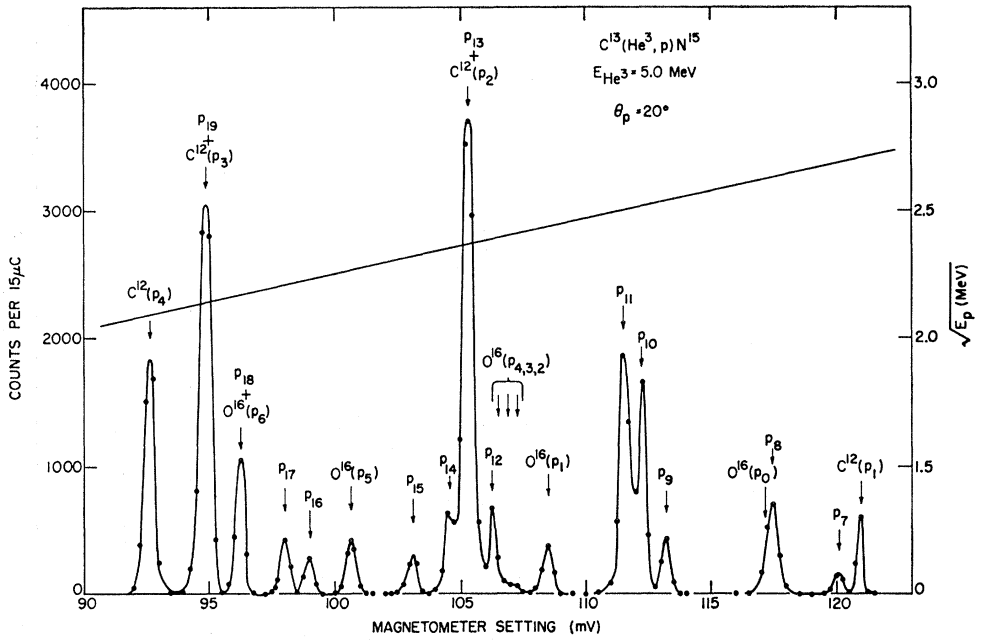

FIG. 3. Proton momentum profile for the $C^{13}(He^3,p)N^{15}$ reaction at an incident beam energy of 5 MeV and a magnetic-spectrometer angle of 20°. Proton groups from O^{16} and C^{12} in the target are labeled by the target nucleus.

upward and was defined by adjustable slits at the entrance and exit. An entrance aperture 2 in. vertical by 0.5 in. horizontal, located 8 in. from the target, and a 0.25 in. vertical exit slit were used. The magnetic field strength in the spectrometer was measured by a constant-temperature Hall-voltage probe. Aluminum foils were positioned in front of the detector at the exit of the magnet in order to allow protons leading to the level of interest in N^{15} to be detected, but to prevent heavier particles from competing reactions from reaching the detector.

The reaction $C^{13}(He^3,p)N^{15}$ has a ground-state Q value of 10.67 MeV,[7] so that for modest bombarding energies all levels below 11 MeV can be populated. Proton-singles spectra were taken for incident He^3 energies of 2 and 5 MeV for spectrometer angles of 20° and 120°. Figures 2 and 3 show typical spectra of proton counts versus Hall voltage, which is proportional to the magnetic field (i.e., to the square root of the proton energy). The straight lines in the figures give the calibration of Hall voltage versus the square root of the proton energy. Proton groups from the $C^{12}(He^3,p)N^{14}$ and $O^{16}(He^3,p)F^{18}$ reactions from the remnant C^{12} and the ubiquitous oxygen contamination in the target are identified in the various spectra.

Data were taken at angles as far forward and backward as practical, in order to sample forward or backward peaking in the angular distributions and to take maximum advantage of the reaction kinematics in separating the particle groups of interest from those emanating from contaminant elements. In all but one case it was possible at one of the four combinations of angle and energy to clearly resolve the groups leading to levels in N^{15} from nearby contaminant peaks and to obtain a useful yield for performing coincidence measurements. The exception was $p_{12}(E_x=9.76$ MeV) which is obscured by protons from the $O^{16}(He^3,p)F^{18}$ reaction at 2 MeV and 20° and which has only a small yield at the other energy-angle combinations. Since its distribution seemed to be peaked forward at 2 MeV, the p_{12} group was measured at 90° where its relative yield was found to be three times greater than at 120°.

To obtain coincident γ-ray spectra, a spectrometer angle and incident energy were chosen, and the spectrometer magnetic field was adjusted for the proton group leading to the level of interest in N^{15}. A coincident γ-ray spectrum and a spectrum of accidental coincidences for later subtraction from the former were accumulated simultaneously in the two halves of a 512-channel analyzer. Singles spectra were taken before and after each run for calibration purposes. A typical singles spectrum, taken at 2-MeV incident energy, is shown in Fig. 4. The prominent γ-ray peaks are identified and the straight line gives the γ-ray energy calibration. During the coincidence runs the prominent 2.31-MeV γ-ray peak from the $C^{12}(He^3,p\gamma)N^{14}$ reaction was used for gain stabilization.[34] In order to minimize pile-up in the γ-ray singles spectrum, beam currents of less than 0.3 μA at 2 MeV (<0.07 μA at 5 MeV) were used. Proton-singles counting rates at these beam currents were at most a few counts per second, while real coinci-

[34] A "Spectrastat," obtained from Cosmic Radiation Laboratories Inc., Bellport, New York, was used for gain stabilization.

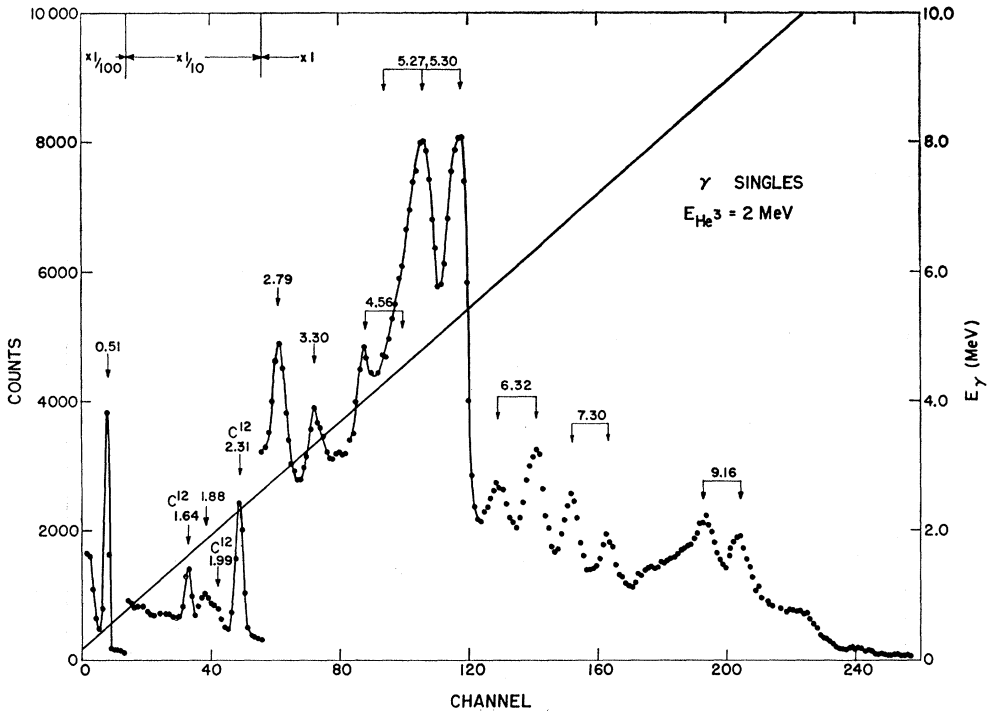

FIG. 4. γ-ray singles spectrum for a 2-MeV He^3 beam on a thin self-supporting carbon foil enriched to 60% C^{13}. γ rays from C^{12} in the target are labeled by the target nucleus.

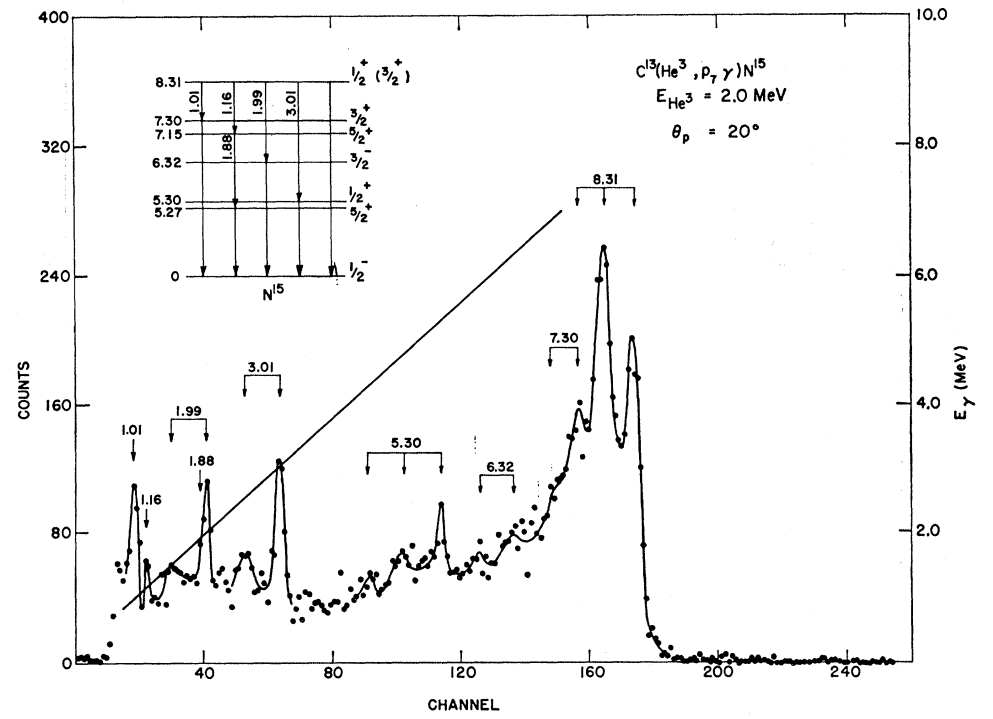

FIG. 5. γ-ray coincidence spectrum for the 8.31-MeV level in N^{15} from the $C^{13}(He^3,p\gamma)N^{15}$ reaction. The decay scheme deduced from the spectrum is shown as an insert.

dence counting rates were about $\frac{1}{5}$ of the proton singles rates. Accidental counting rates were in all cases less than 5% of the real coincidence counting rates. Coincidence spectra for ten levels in N^{15} between 8.31 and 10.45 MeV are shown in Figs. 5 to 14. The straight lines give the γ-ray energy calibrations, and the decay schemes deduced from the spectra are indicated on the figures.

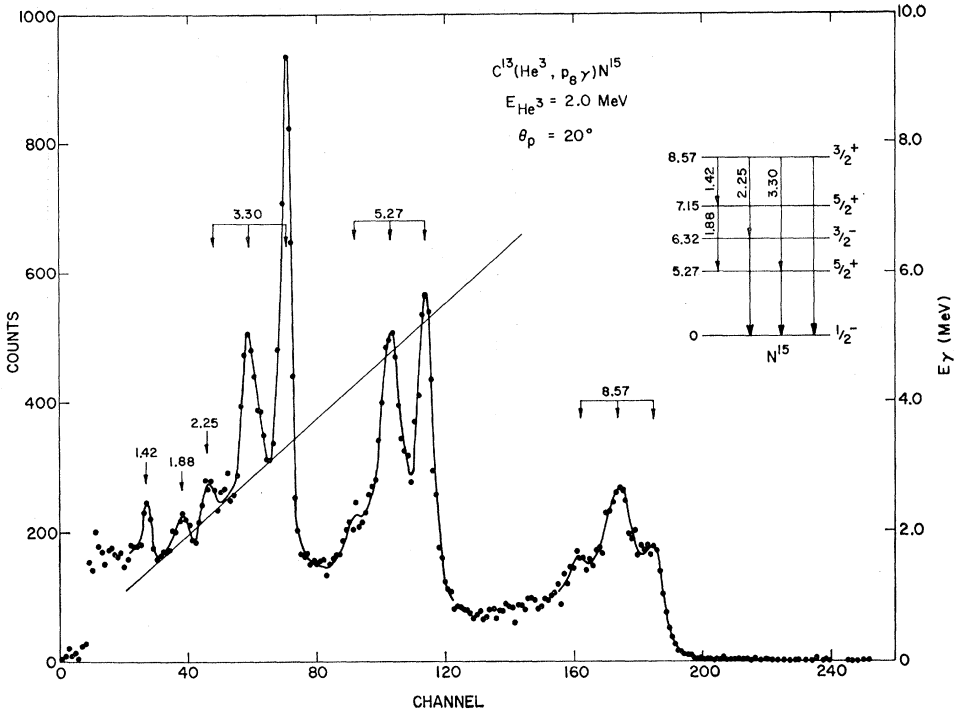

FIG. 6. γ-ray coincidence spectrum for the 8.57-MeV level in N^{15} from the $C^{13}(He^3,p\gamma)N^{15}$ reaction. The decay scheme deduced from the spectrum is shown as an insert.

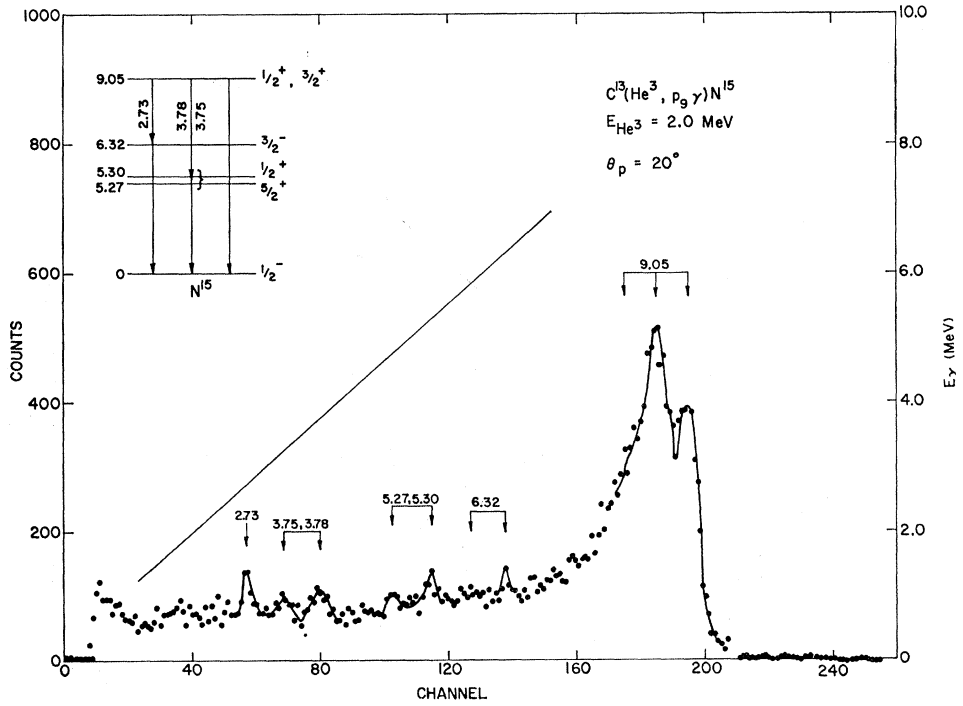

FIG. 7. γ-ray coincidence spectrum for the 9.05-MeV level in N^{15} from the $C^{13}(He^3,p\gamma)N^{15}$ reaction. The decay scheme deduced from the spectrum is shown as an insert.

B. Results

1. Energy Levels in N^{15}

The proton-singles spectra (Figs. 2 and 3) were obtained with a proton-energy resolution of about 40 keV (full width at half-maximum, FWHM). Thus, the doublet of N^{15} energy levels at excitation energies of 5.27 and 5.30 MeV was unresolved, but all other levels were clearly separated. Firm evidence was obtained for a triplet of levels at 9.05, 9.16, and 9.22 MeV as well as

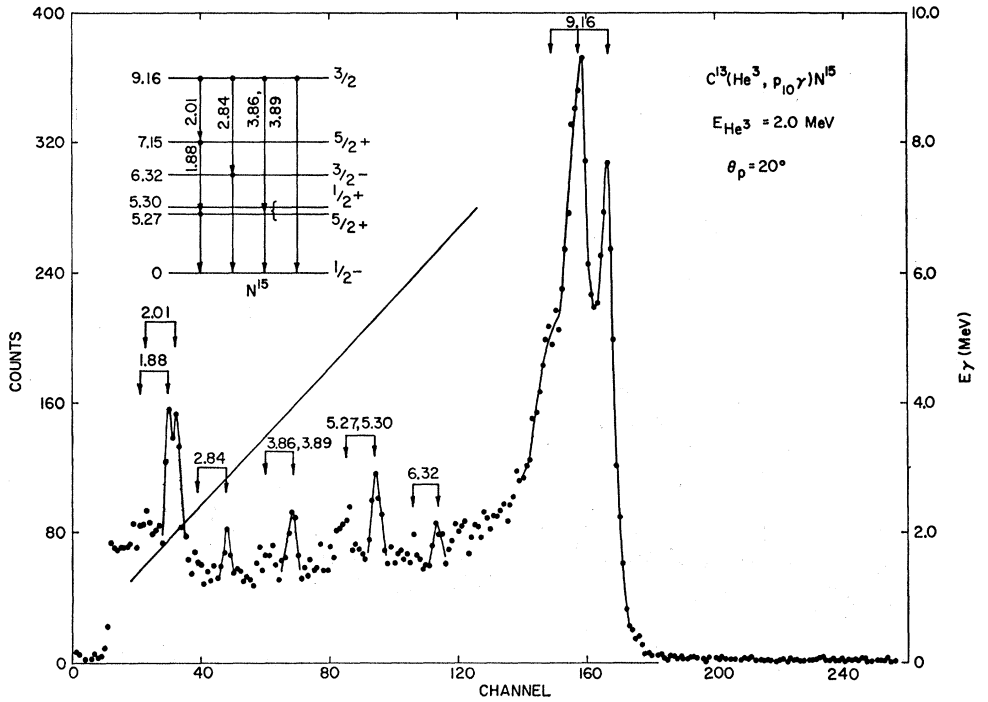

FIG. 8. γ-ray coincidence spectrum for the 9.16-MeV level in N^{15} from the $C^{13}(He^3,p\gamma)N^{15}$ reaction. The decay scheme deduced from the spectrum is shown as an insert.

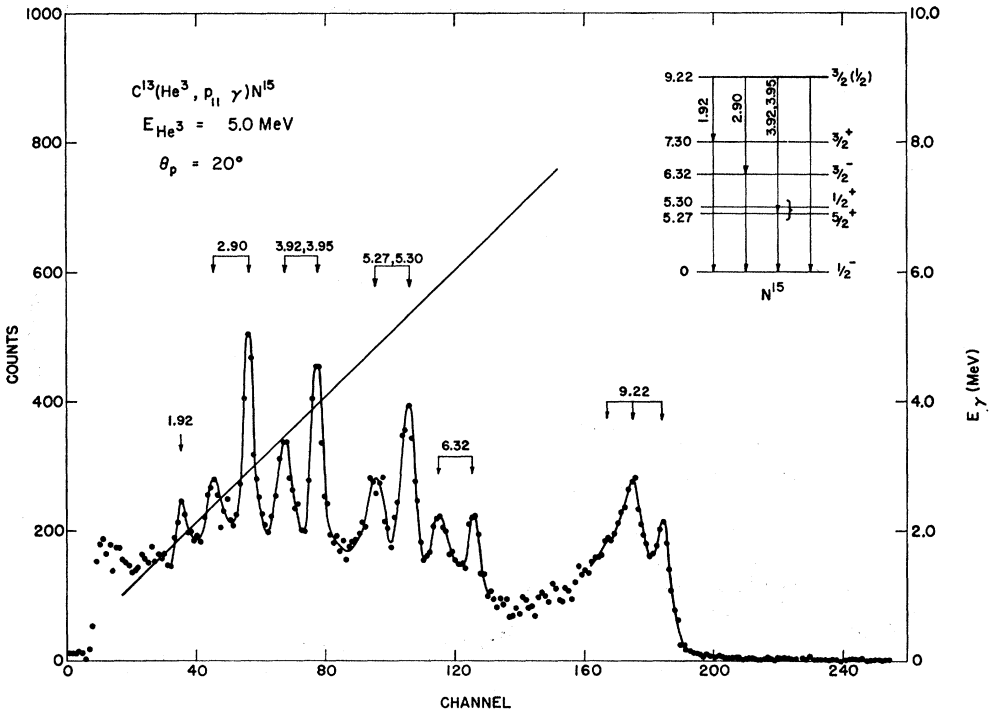

FIG. 9. γ-ray coincidence spectrum for the 9.22-MeV level in N^{15} from the $C^{13}(He^3,p\gamma)N^{15}$ reaction. The decay scheme deduced from the spectrum is shown as an insert.

for quadruplets at 9.76, 9.83, 9.93, and 10.07 MeV and at 10.45, 10.54, 10.70, and 10.80 MeV. Since the proton separation energy of N^{15} is 10.21 MeV,[7] the latter four levels can decay by proton emission to C^{14}. Only the levels at 10.45 and 10.80 MeV are known to have sizeable γ-ray widths,[9,16–18,26] and of these only the former was produced with sufficient yield for coincidence measurements in the $C^{13}(He^3,p\gamma)N^{15}$ reaction at the available incident He^3 energies. No evidence was found for levels at 8.74, 9.60, and 8.64 MeV (doubtful) as re-

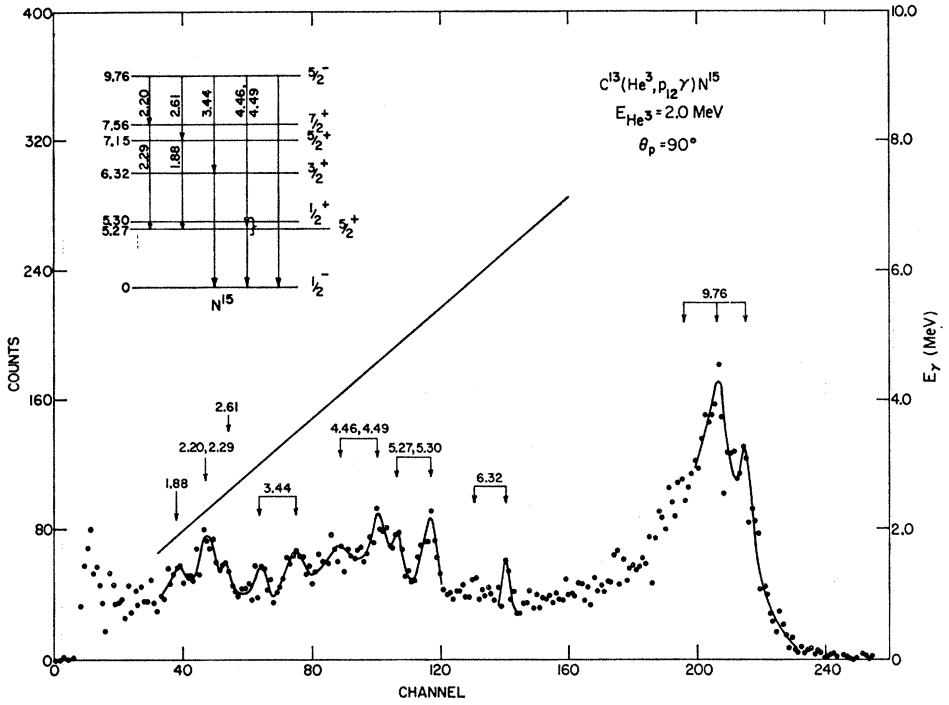

FIG. 10. γ-ray coincidence spectrum for the 9.76-MeV level in N^{15} from the $C^{13}(He^3,p\gamma)N^{15}$ reaction. The decay scheme deduced from the spectrum is shown as an insert.

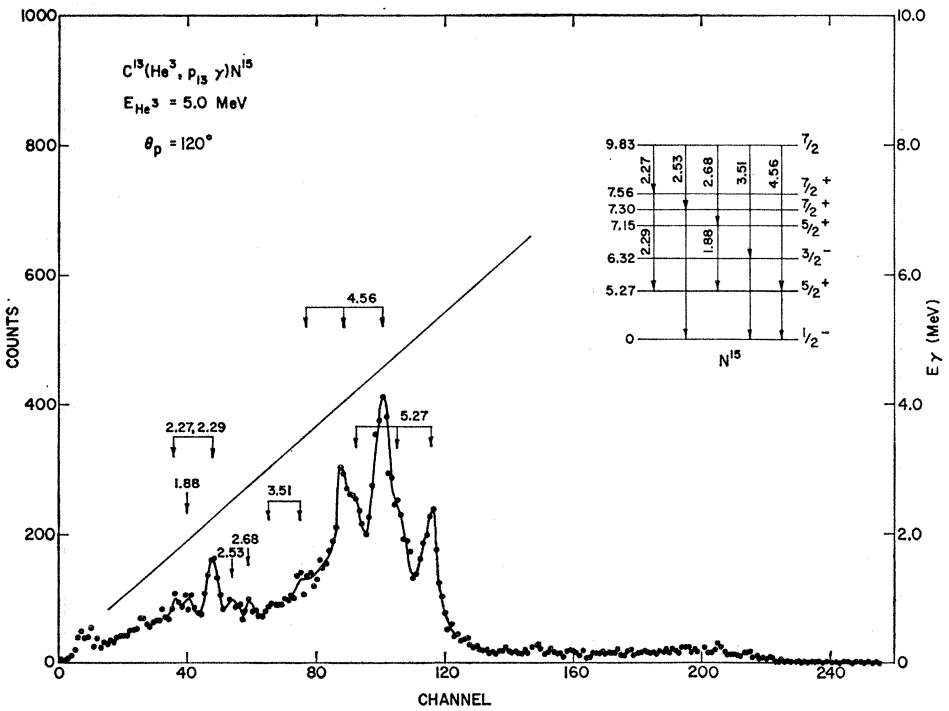

FIG. 11. γ-ray coincidence spectrum for the 9.83-MeV level in N^{15} from the $C^{13}(He^3,p\gamma)N^{15}$ reaction. The decay scheme deduced from the spectrum is shown as an insert.

ported in the $N^{14}(d,p)N^{15}$ reaction by Kashy *et al.*[35] Recently published results[14] of magnetic-spectrograph measurements for the $N^{14}(d,p)N^{15}$ and $C^{13}(He^3,p)N^{15}$ reactions also gave no evidence for these three levels. In the present measurements no evidence was found for a level at 10.94 MeV for which "strong but nonconclusive" evidence was reported in the $C^{13}(He^3,p\gamma)N^{15}$

[35] E. Kashy, A. Sperduto, F. P. Gibson, and A. M. Hoogenboom, Massachusetts Institute of Technology Laboratory for Nuclear Science Progress Report, 1961 (unpublished).

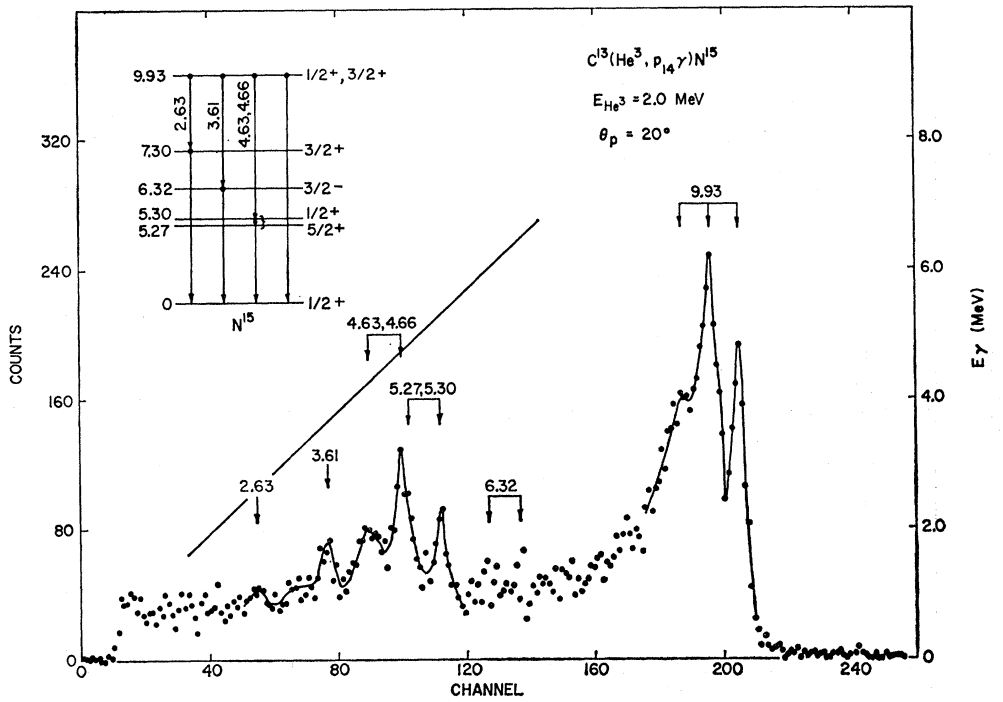

FIG. 12. γ-ray coincidence spectrum for the 9.93-MeV level in N^{15} from the $C^{13}(He^3,p\gamma)N^{15}$ reaction. The decay scheme deduced from the spectrum is shown as an insert.

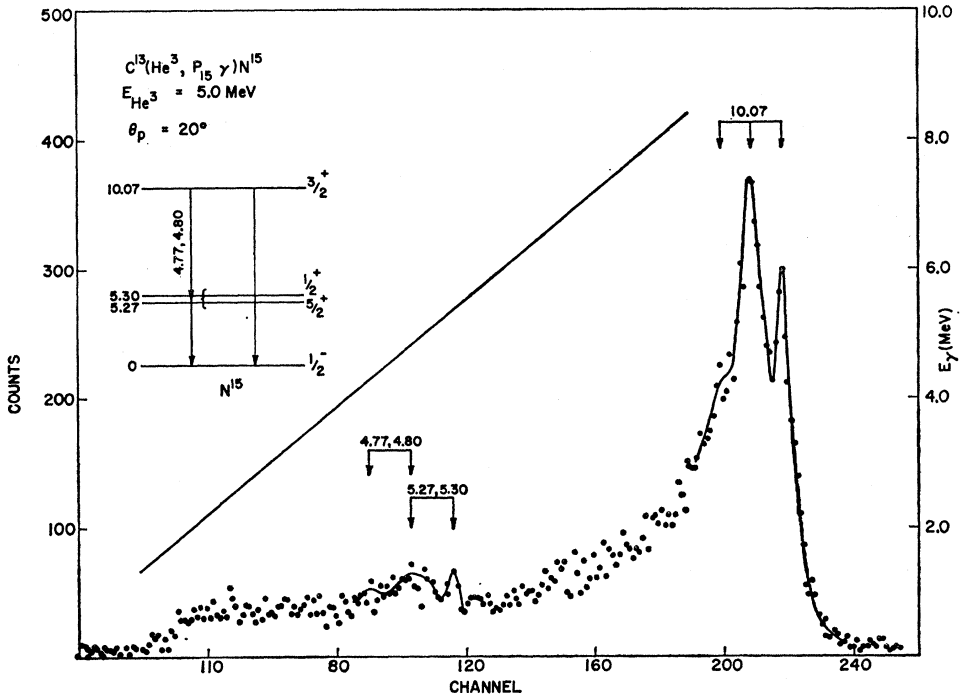

FIG. 13. γ-ray coincidence spectrum for the 10.07-MeV level in N^{15} from the $C^{13}(He^3,p\gamma)N^{15}$ reaction. The decay scheme deduced from the spectrum is shown as an insert.

measurements of Warburton and Olness.[26] By using as calibration points various excited-state energies which had been measured previously,[9,15] the excitation energies of levels at 9.05, 9.22, 9.83, and 10.07 MeV were determined. Table I gives the results for each value of the incident energy and spectrometer angle at which the levels were observed and the mean value of the excitation energy for each level. Contributions to the uncer-

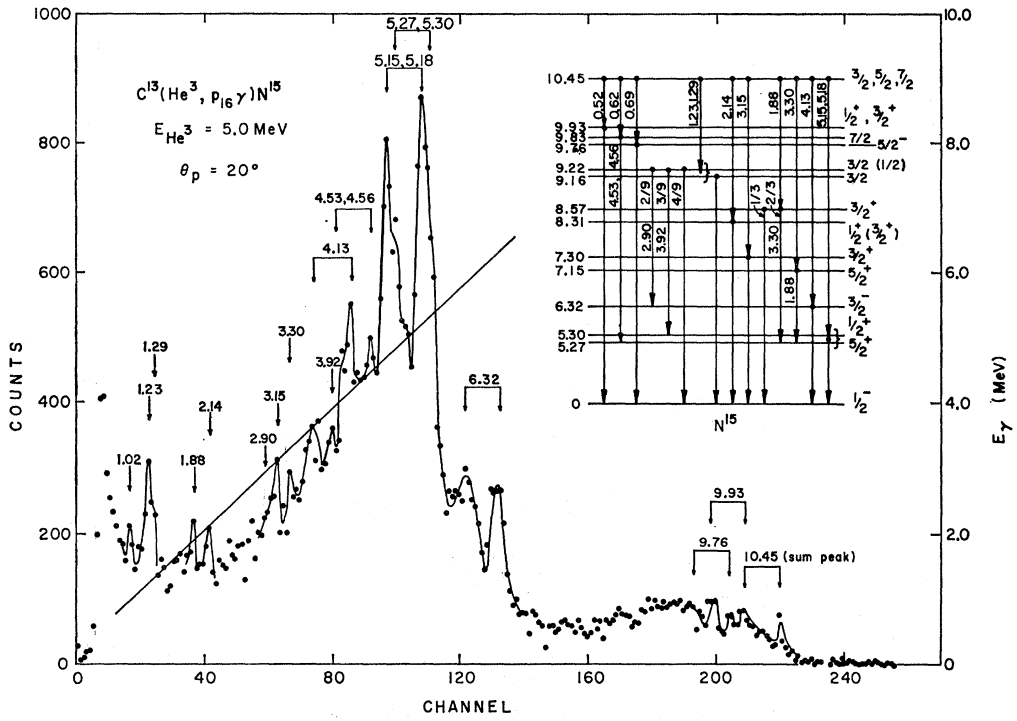

FIG. 14. γ-ray coincidence spectrum for the 10.45-MeV level in N^{15} from the $C^{13}(He^3,p\gamma)N^{15}$ reaction. The decay scheme deduced from the spectrum is shown as an insert.

tainty in these values due to the uncertainty of the peak position and to the uncertainties in the calibration energies are comparable. Precise values for some levels could not be obtained at certain spectrometer angles and incident energies because of interference from proton peaks due to contaminants. Table I also gives the mean value of the excitation energy calculated from the results of Gallman *et al.*[14] for the $N^{14}(d,p)N^{15}$ and $C^{13}(He^3,p)N^{15}$ reactions by averaging columns 3 and 7 of Table II in Ref. 14. The present energy determinations are in good agreement with these results. The final averages in Table I include the results of Warburton *et al.*,[9] Gallmann *et al.*,[14] and the present work.

2. γ-Ray Branching Ratios

Branching ratios were extracted from the coincident γ-ray spectra using previously measured efficiencies and peak-to-total ratios for the 5-in.-diam×5-in. NaI(Tl) crystal in the same experimental geometry.[30] The peak-to-total ratio measurements also provided monoenergetic γ-ray line shapes from 0.432 to 9.17 MeV, which were used in analyzing the coincidence spectra. The branching ratios obtained for the levels in N^{15} between 8.31 and 10.45 MeV are given in Table II together with a summary of previous measurements. The uncertainties given for the branching ratios include

TABLE I. Excitation energies in N^{15} from $C^{13}(He^3,p)N^{15}$ proton-singles measurements.

Proton group	θ_p (deg)	Excitation energy (MeV) 2 MeV	5 MeV	Mean excitation energy (MeV) Present data	Gallmann *et al.*[a]	Average[b]
p_9	20	9.054±0.006	...	9.054±0.004	9.056±0.004	9.054±0.002
	120	9.053±0.006	9.054±0.006			
p_{11}	20	9.224±0.006	9.225±0.006	9.225±0.003	9.226±0.004	9.225±0.002
	120	9.225±0.006	9.227±0.006			
p_{13}	120	9.827±0.005	9.831±0.006	9.829±0.004	9.829±0.004	9.829±0.003
p_{15}	20	10.072±0.006	10.072±0.006	10.072±0.004	10.068±0.005	10.072±0.003
	20	10.071±0.006	...			

[a] Reference 14.
[b] Average of results from Refs. 9, 14, and the present work.

TABLE II. Branching ratios in N^{15} from the $C^{13}(He^3,p\gamma)N^{15}$ reaction.

E_x (MeV)	E_f (MeV)	E_γ (MeV)	Present data (%)	Previous data (%)[a]
8.31	0	8.31	79.1±1.9	78±3
	5.27	3.04	10.9±1.3	<3
	5.30	3.01		11±2
	6.32	1.99	4.4±1.0	8.8±2
	7.15	1.16	1.2±0.6	<1
	7.30	1.01	4.4±0.7	2.2±0.4
8.57	0	8.57	33.4±2.0	32±3
	5.27	3.30	61.6±2.0	65±3
	5.30	3.27		<12
	6.32	2.25	1.4±0.6	3±1
	7.15	1.42	3.6±0.5	<4
	7.30	1.27	<1	<0.7
	7.56	1.01		<3
9.05	0	9.05	91.6±0.9	91±3
	5.3[b]	3.75	4.7±0.7	3.8±1
	6.32	2.73	3.7±0.5	4±1
	7.15	1.90	<1	<10
	7.30	1.75		1.2±0.4
	7.56	1.49		<2
	8.31	0.74	...	<0.5
9.16	0	9.16	86.5±4.5	56±10
	5.3[b]	3.8	4.9±1.8	7±3
	6.32	2.84	2.5±0.8	10±5
	7.15	2.01	6.1±1.8	23±5
	7.30	7.30[c]	<2	4±2
	7.56	1.60	<1	<5
	8.31	0.85		<0.5
9.22	0	9.22	41.5±2.2	<30
	5.27	3.95	31.2±1.7	≲25
	5.30	3.92		100
	6.32	2.90	24.7±1.5	<25
	7.15	2.07	<1	<30
	7.30	1.92	2.6±0.7	<30
	7.56	1.66	<1	<20
	8.31	0.91		<5
9.76	0	9.76	81.5±2.8	100
	5.3[b]	4.5	7.5±1.5	<10
	6.32	3.44	3.7±0.8	<5
	7.15	2.61	2.3±0.5	<10
	7.30	7.30[c]	<2	<3
	7.56	2.20	5.0±0.6	<10
	8.31	1.45	<1	<2
	8.57	1.19	<2	<2
9.83	0	9.83	<4	<30
	5.27	4.56	84.4±1.8	100
	5.30	4.53		<15
	6.32	3.51	2.2±0.9	<15
	7.15	2.68	2.4±1.1	<10
	7.30	2.53	3.7±0.9	<10
	7.56	2.27	7.3±1.0	<10
	8.31	1.52	<1	...
	8.57	1.26		...
9.93	0	9.93	77.6±1.9	80±10
	5.3[b]	4.6	15.4±1.5	10±10
	6.32	3.61	4.9±1.2	10±10
	7.15	2.78	<1	<10
	7.30	2.63	2.1±0.8	<3
	7.56	2.37	<1	<10
	8.31	1.62		<2
	8.57	1.36		<2
10.07	0	10.07	96.0±0.7	94±4
	5.3[b]	4.8	4.0±0.7	6±2
	6.32	3.75	<1	<2 (to 8.31)
	⋮	⋮		
	9.22	0.85[c]		
	9.83	4.56		<3 (to 8.57)
10.45	0	10.45	<4	<4
	5.3[b]	5.2	62.4±2.4	70±5
	6.32	4.13	14.7±1.6	24±5
	7.15	3.30	1.6±0.6	<6
	8.57	1.88		
	7.30	3.15	2.3±0.8	
	7.56	2.89	<1	
	8.31	2.14	1.5±0.5	6±3
	9.05	1.40	<1	
	9.16	1.29	5.0±0.5	
	9.22	1.23		
	9.76	9.76[c]	1.6±0.7	
	9.83	4.56[c]	2.2±1.5	
	9.93	9.93[c]	3.7±1.1	
	10.07	10.07[c]	<4	

[a] References 9 and 26.
[b] Decay to 5.30–5.27 MeV doublet, not resolved.
[c] Decay to E_f not observed, branching ratio obtained from cascade γ ray listed.

statistical errors and uncertainties in the values of the efficiencies and peak-to-total ratios,[30] but they do not include possible effects of unknown angular correlations. Although the large solid angle covered by the 5-in.-diam×5-in. NaI crystal (about 4.2 sr) tends to integrate over correlations, effects as large as 10% due to correlations have been observed.[30] Since the stated uncertainties on the branching ratios are significantly smaller than previous measurements, the procedure used in the error analysis is given in an Appendix.

III. THEORETICAL ELECTROMAGNETIC TRANSITION STRENGTHS

A. Model for Low-Lying Excited Levels in N^{15}

The individual-particle model has been used successfully in predicting the excitation energies, spins, and parities of low-lying levels for nuclei in the mass region $5 \leq A < 20$.[2,4,36,37] In this model the actual, unknown wave function ψ_ν for a nucleus in a state of excitation energy E_ν is expanded in terms of a complete orthonormal set of known wave functions φ_i,

$$\psi_\nu = \sum_i a_{\nu i} \varphi_i. \quad (1)$$

In principle, any complete orthonormal set may be used, but to make the work involved in calculating nuclear matrix elements manageable, it is necessary to to choose a set $\{\varphi_i\}$ which is a reasonably good approximation of the actual wave functions ψ_ν so that all but a few of the terms in the above expansion are negligibly

[36] J. P. Elliott and B. H. Flowers, Proc. Roy. Soc. (London) **A229**, 536 (1955).
[37] J. P. Elliott and A. M. Lane, in *Handbuch der Physik*, edited by S. Flügge (Springer-Verlag, Berlin, 1957), Vol. 39, p. 241.

small. At the same time the wave functions in the basis set $\{\varphi_i\}$ should be simple enough that they can be used conveniently in calculations. It is customary to use single-particle shell-model wave functions as the basis set. The number of non-negligible coefficients $a_{\nu i}$ which must then be retained in the expansion is, in fact, a measure of how good the shell model is for low-lying levels in this mass region.

Kurath[2] has used shell-model wave functions to calculate the lowest-order normal-parity levels for nuclei with $5 \leq A \leq 15$, allowing only excitations within the $1p$ shell. Since N^{15} has only a single hole in the $1p$ shell, this produces only two levels, with $J^\pi = \frac{1}{2}^-$ and $\frac{3}{2}^-$, corresponding to the ground state and the excited level at 6.32 MeV, respectively. Levels arising from the next lowest excitations in the shell model involve configurations which result from raising a nucleon from the $1s$ core to complete the $1p$ shell, or from raising a $1p$ nucleon into the $2s$-$1d$ shell. These configurations give states of even parity and therefore cannot interfere with the odd-parity states of lowest order. Halbert and French[3,4] have used these next-order configurations as the basis set $\{\varphi_i\}$ for an individual-particle-model calculation to obtain properties of theoretical even-parity levels for $A=15$. The results for the first seven even-parity levels are shown in Fig. 1, and identifications or tentative identifications (dashed lines) with levels in N^{15} and its mirror nucleus O^{15} are indicated. The predominant single-particle configuration and the percent of the intensity of the total wave function in this configuration are given for each level.[3,4] The theoretical energies are normalized relative to a value of 5.28 MeV for the first $\frac{5}{2}^+$ level in N^{15}. The number of theoretical levels and their spins and parities agree well with the experimental energy levels up to 9 MeV in N^{15}, although there is some crossing in the order of the levels. Better agreement in this regard could probably be obtained by varying the parameters, which was not done at the time (1956) because of the effort involved in diagonalizing the matrices. (Elliott and Flowers[36] in individual-particle-model calculations for nuclei with $A=18$ and 19 observed crossing of levels as the depth of the central potential was varied.) Halbert has used the wave functions obtained to calculate other properties of the levels, notably neutron reduced widths, and has obtained reasonable agreement with experimental values from the $N^{14}(d,p)N^{15}$ reaction.[3]

B. Branching Ratio Calculations

Halbert[3] has derived an expression for $E1$ ground-state transition strengths from theoretical even-parity levels for $A=15$. This derivation has been generalized to obtain expressions for electromagnetic transitions of all multipolarities between theoretical levels for mass-15 nuclei.[38] For the even-parity levels, Halbert's individual-particle-model wave functions were used. The odd-parity ground-state and 6.32-MeV level were taken to be pure single-particle states, with a single hole in the $1p$ shell coupled to $J=\frac{1}{2}$ and $\frac{3}{2}$, respectively. The resulting expressions for the matrix elements of the electromagnetic transitions contain a coherent sum of terms involving transitions between the single-particle harmonic-oscillator states used by Halbert and French[3,4] in the expansion for their theoretical levels of even parity.

Of the ten levels for which Halbert has given wave functions, the seven lowest in energy are identified with levels in N^{15} as shown in Fig. 1. The next two levels have $T=\frac{3}{2}$. The remaining wave function is for a third $J=\frac{1}{2}$, $T=\frac{1}{2}$ level. Although this level has a model energy above 12 MeV (and thus is not shown in Fig. 1), it appears reasonable from Fig. 1 to look for an experimental level lower in energy, around 9 or 10 MeV perhaps, which can be identified with this theoretical level. Recall that the theoretical levels were arbitrarily normalized to equate the energy of the first $\frac{5}{2}^+$ theoretical level with that of the first excited level in N^{15}. If the normalization were made instead between the centers of gravity of the seven theoretical levels shown in Fig. 1 and the corresponding experimental levels in N^{15}, the theoretical energies would be lowered considerably. Therefore, from the spins and parities shown in Fig. 1, the levels at 9.05 and 9.93 MeV in N^{15} are likely candidates for identification with the third $\frac{1}{2}^+$ theoretical level.

To determine the usefulness of comparing theoretical transition strengths to the experimental branching ratios, calculations were made for the second $\frac{1}{2}^+$ level and the second $\frac{3}{2}^+$ level, identified with the experimental levels in N^{15} at 8.31 and 8.57 MeV, respectively, as well as for the third $\frac{1}{2}^+$ level, assuming excitation energies of 9.05 and 9.93 MeV. Terms that were at least an order of magnitude smaller than the leading term in the matrix element were neglected; therefore the theoretical transition strengths are accurate to about 10%. The results of the theoretical calculations are compared in Table III with the experimental branching ratios. No attempt has been made to average the present branching ratios with previous results because it is not clear how the errors were assigned in the previous analyses. For example, if the branching ratios are constrained to sum to 100% and only two branches are observed, then the percentage errors on the two branches must be identical (see Appendix). It is noted in Table II that this condition is true for the 10.07-MeV state (where only two branches are observed) for the present data, but not for the previous data. The agreement between theory and experiment in Table III is quite good for the 8.31- and 8.57-MeV levels. For example, the enhanced strength of the 8.57–5.27-MeV decay predicted by the model leads to a branching ratio which is in good agreement with experiment. Also the decays of the 8.31- and 8.57-MeV levels to the 5.27- and 5.30-MeV

[38] G. W. Phillips, Ph.D. thesis, University of Maryland, 1966 (unpublished).

TABLE III. Comparison of experimental branching ratios to theoretical transition strengths.

Initial level[a]		Final level[a]			Theoretical	Branching ratios	
J^π	E_x (MeV)	J^π	E_f (MeV)	Assumed multipolarity	transition strength (Weisskopf units)	Theory	Experiment (present data)
$\frac{1}{2}_b^+$	8.31	$\frac{1}{2}^-$	0	$E1$	0.0015	79.6	79.1±1.9
		$\frac{5}{2}_a^+$	5.27	$E2$	Very weak	<0.1	10.9±1.3
		$\frac{1}{2}_a^+$	5.30	$M1$	0.0068	8.5	
		$\frac{3}{2}^-$	6.32	$E1$	0.016	11.2	4.4±1.0
		$\frac{5}{2}_b^+$	7.15	$E2$	Very weak	<0.1	1.2±0.6
		$\frac{3}{2}_a^+$	7.30	$M1$	0.15	0.7	4.4±1.0
$\frac{3}{2}_b^+$	8.57	$\frac{1}{2}^-$	0	$E1$	0.0018	34.2	33.4±2.0
		$\frac{5}{2}_a^+$	5.27	$M1$	1.1	58.7	61.6±2.0
		$\frac{1}{2}_a^+$	5.30	$M1$	Very weak	<0.1	
		$\frac{3}{2}^-$	6.32	$E1$	0.018	6.3	1.4±0.6
		$\frac{5}{2}_b^+$	7.15	$M1$	0.19	0.8	3.6±0.5
		$\frac{3}{2}_a^+$	7.30	$M1$	Very weak	<0.1	<1
$\frac{1}{2}_c^+$	9.05	$\frac{1}{2}^-$	0	$E1$	0.017	96.3	91.6±0.9
		$\frac{5}{2}_a^+$	5.27	$E2$	Very weak	<0.1	4.7±0.7
		$\frac{1}{2}_a^+$	5.30	$M1$	0.012	2.2	
		$\frac{3}{2}^-$	6.32	$E1$	0.00087	1.4	3.7±0.5
		$\frac{5}{2}_b^+$	7.15	$E2$	Very weak	<0.1	<1
		$\frac{3}{2}_a^+$	7.30	$M1$	0.0064	0.1	
$\frac{1}{2}_c^+$	9.93	$\frac{1}{2}^-$	0	$E1$	0.0017	94.3	77.6±1.9
		$\frac{5}{2}_a^+$	5.27	$E2$	Very weak	<0.1	15.4±1.5
		$\frac{1}{2}_a^+$	5.30	$M1$	0.012	3.0	
		$\frac{3}{2}^-$	6.32	$E1$	0.00087	2.3	4.9±1.2
		$\frac{5}{2}_b^+$	7.15	$E2$	Very weak	<0.1	<1
		$\frac{3}{2}_a^+$	7.30	$M1$	0.0064	0.4	2.1±0.8

[a] The sequence of theoretical levels of the same J^π is indicated by subscripts of small letters.

states have been experimentally resolved (see Table II) and are in good agreement with the theoretical calculations. Thus, an attempt to identify the third $\frac{1}{2}^+$ theoretical level with either the 9.05- or 9.93-MeV experimental levels by comparing the theoretical and experimental branching ratios is meaningful. It can be seen from Table III that the agreement is quite good for the 9.05-MeV level. However, the branching ratios to the ground state are in poor agreement for the 9.93-MeV level, and the theoretical and experimental branching ratios for the decays to the first $\frac{1}{2}^+$ level (5.30 MeV) and the first $\frac{3}{2}^+$ level (7.30 MeV) differ by a factor of 5. Thus, identification of the third $\frac{1}{2}^+$ theoretical level with the level at 9.05 MeV seems more likely.

IV. PROTON–γ-RAY ANGULAR CORRELATIONS

A. Correlation Theory

Proton–γ-ray angular correlations in the C^{13}-$(He^3,p\gamma)N^{15}$ reaction were measured by detecting the protons emitted at 0° with respect to the beam direction. This geometry has been treated theoretically by Litherland and Ferguson,[39,40] who refer to this experimental configuration as Method II. The angular correlation in this geometry for a subsequent γ-ray decay $a \rightarrow b$ from a level with spin a to a level with spin b has the form, in the notation of Poletti and Warburton,[41]

$$W(\theta)=\sum_k \rho_k(a)F_k(ab)Q_kP_k(\cos\theta) \qquad (2)$$

for a γ ray detected at an angle θ, where the sum on k runs over even integers beginning with zero and does not exceed $2a$. The $P_k(\cos\theta)$ are Legendre polynomials. The Q_k are attenuation coefficients for a detector of finite size normalized so that $Q_0=1$. Tables of Q_2 and Q_4 for cylindrical detectors have been given by Ferguson.[40] The statistical tensors $\rho_k(a)$ are defined by Poletti and Warburton[41] in terms of the population parameters $P(\alpha)$ for states of magnetic quantum number α. For the $C^{13}(He^3,p)N^{15*}$ reaction in the geometry of Method II, the excited state in N^{15} has $|\alpha| \leq \frac{3}{2}$. Since the initial state is unpolarized and the polarization of the outgoing particle is not detected, $P(\alpha)=P(-\alpha)$. The $F_k(ab)$ are defined in terms of the multipole mixing ratio x and coefficients $F_k(LL'ba)$ which have been tabulated by Poletti and Warburton.[41]

The theoretical expressions for the angular correlations were used to analyze the measured angular correla-

[39] A. E. Litherland and A. J. Ferguson, Can. J. Phys. **39**, 788 (1961).

[40] A. J. Ferguson, *Angular Correlation Methods in Gamma-Ray Spectroscopy* (North-Holland Publishing Company, Inc., Amsterdam, 1965).

[41] A. R. Poletti and E. K. Warburton, Phys. Rev. **137**, B595 (1965).

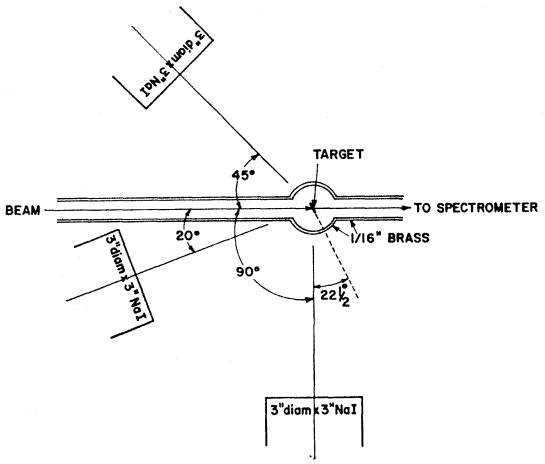

FIG. 15. Experimental geometry for the proton–γ-ray angular-correlation measurements.

tions by treating the population parameters $P(\frac{1}{2})$ and $P(\frac{3}{2})$, which are constrained on physical grounds to be greater than or equal to zero, as unknown parameters to be determined by a least-squares analysis of the experimental data. The spin of the excited state in N^{15} was treated as an unknown discrete parameter, and the most probable value was determined by performing a χ^2 analysis for different spin values, where

$$\chi^2=\frac{\sum_i [Y(\theta_i)-W(\theta_i)]^2}{\Delta^2(\theta_i)} \tag{3}$$

for a yield $Y(\theta_i)$ at an angle θ_i with an uncertainty $\Delta(\theta_i)$. χ^2 analyses were made over the range $-\infty<x<\infty$ for the multipole mixing ratio x. This method of analysis is illustrated in the following section (see also Refs. 41–43).

B. Correlation Measurements

The experimental arrangement used for the angular-correlation measurements is shown in Fig. 15. The protons were analyzed by the magnetic spectrometer and were detected by a solid-state detector at the exit of the magnet. The entrance slits were opened to the maximum spectrometer solid angle of 0.022 sr (2.25 in. vertical by 0.75 in. horizontal), and a 0.25 in. vertical exit slit was used. The target chamber was constructed of a vertical 1.5-in.-diam cylinder intersected horizontally by a rectangular beam tube, 1.5 in. vertical by 0.75 in. horizontal. Because the theoretical correlations depend only on even powers of $\cos\theta$, we have $W(\theta)=W(-\theta)$, and it is necessary to take data only in one quadrant. Three 3-in.-diam×3-in. NaI(Tl) γ-ray detectors were placed with their axes at angles relative to the beam direction of 90°, 135°, and 160° (chosen as close as practical to 180°) and at a distance of 6.6 in. from the center of the target (measured from the face of the crystal). The target was placed so that the normal to the target plane bisected the angle between the 90° and 135° counters (see Fig. 15).

To minimize γ-ray absorption, the walls of the chamber and beam tube were constructed from $\frac{1}{16}$ in. brass, but at 160° (and to a lesser extent at 135°) some of the γ rays reaching the detector had to pass through the beam-tube wall at an angle, increasing the probability of absorption. To determine the proper correction for this effect, the angular distribution was measured for the isotropic γ ray from the 3.56-MeV level in Li^6, which decays entirely to the ground state and is strongly resonant at 2.56 MeV in the $Be^9(p,\alpha\gamma)Li^6$ reaction.[6,44]

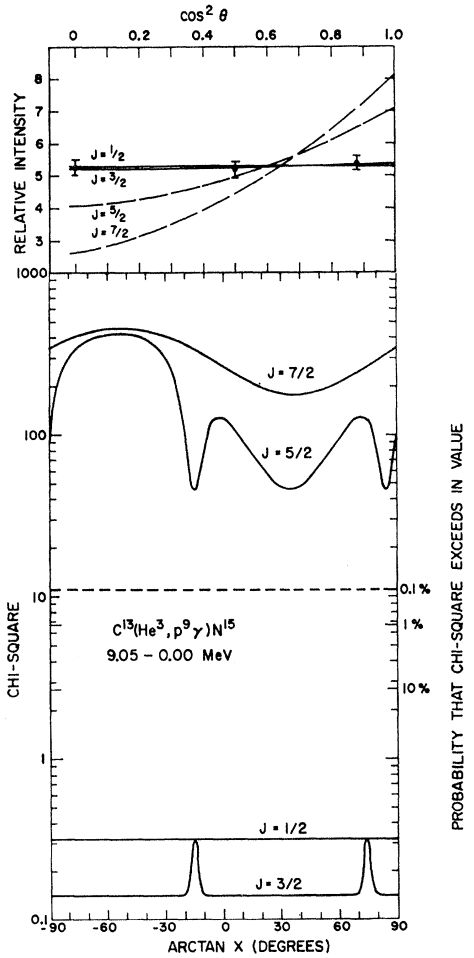

FIG. 16. Plot of χ^2 versus arctan x (the multipole mixing ratio) for the least-square analysis of the proton–γ-ray angular correlation measured for the ground-state decay of the 9.05-MeV level in N^{15} from the $C^{13}(He^3,p\gamma)N^{15}$ reaction. Values of $\frac{1}{2}$, $\frac{3}{2}$, $\frac{5}{2}$, and $\frac{7}{2}$ were assumed for the spin of the 9.05-MeV level. The best theoretical fits to the measured correlation for each value of the spin are also shown.

[42] C. Broude and H. E. Gove, Ann. Phys. (N. Y.) **23**, 71 (1963).
[43] P. W. M. Glaudemanns and P. M. Endt, Nucl. Phys. **42**, 367 (1963).
[44] J. B. Marion, Phys. Rev. **103**, 713 (1956).

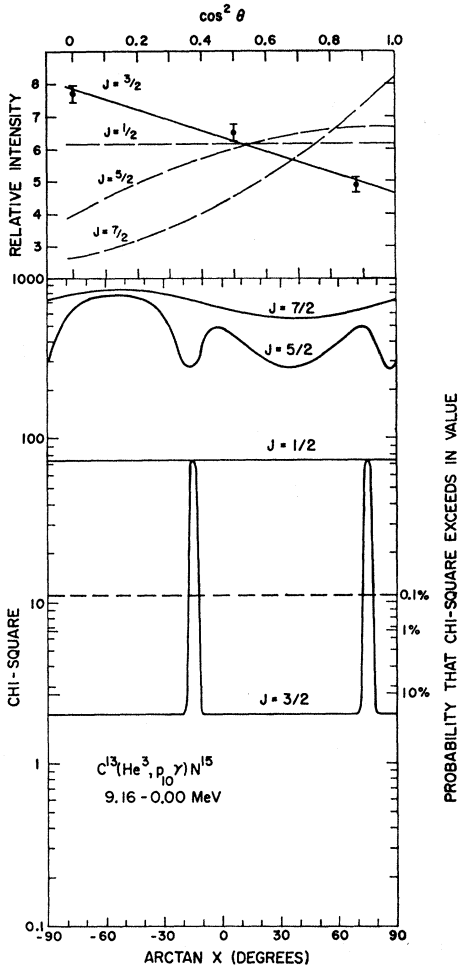

FIG. 17. Plot of χ^2 versus arctan x (the multipole mixing ratio) for the least-square analysis of the proton–γ-ray angular correlation measured for the ground-state decay of the 9.16-MeV level in N^{15} from the $C^{13}(He^3,p\gamma)N^{15}$ reaction. Values of $\frac{1}{2}$, $\frac{3}{2}$, $\frac{5}{2}$, and $\frac{7}{2}$ were assumed for the spin of the 9.16-MeV level. The best theoretical fits to the measured correlation for each value of the spin are also shown.

Corrections were made for the energy dependence of the absorption using tabulated values for the absorption coefficient as a function of γ-ray energy.[45]

Angular correlations for the 9.05-, 9.16-, and 9.22-MeV levels in N^{15} were measured by accumulating in one of three quadrants of a 512-channel analyzer the γ-ray spectrum of each crystal detected in coincidence with the appropriate proton group at the exit of the magnet. Simultaneously, a spectrum of accidental coincidences was accumulated in the fourth quadrant for later subtraction. To stabilize gains in the γ-ray systems as was done with the branching-ratio measurements would have required three gain stabilizers, which were not available. Instead, about every 90 min data accumulation was stopped so that singles γ-ray spectra could be taken for each crystal in an auxiliary 256-channel analyzer, and the amplifier gains were adjusted to keep the strong 2.31-MeV peak from the $C^{12}(He^3,p\gamma)N^{14}$ reaction (Fig. 4) centered in a given channel. In this way gain shifts were held to less than 2%.

Angular-correlation measurements were made for the ground-state decays of the triplet of levels at 9.05, 9.16, and 9.22 MeV in N^{15}, and corrections (of the order of 10%) were included for γ-ray absorption effects. The measured correlations were used in χ^2 analyses as described in the previous section. As the multipole mixing ratio x can have any value from $-\infty$ to ∞, calculations were made for values of arctan$x$ from $-90°$ to $90°$ in $5°$ intervals. In Figs. 16 to 18 are shown the resultant χ^2 values versus arctan$x$ for possible excited-state spins from $J=\frac{1}{2}$ to $\frac{7}{2}$. $J>\frac{7}{2}$ can be eliminated from lifetime considerations.[9,26] Indicated on the figures are the

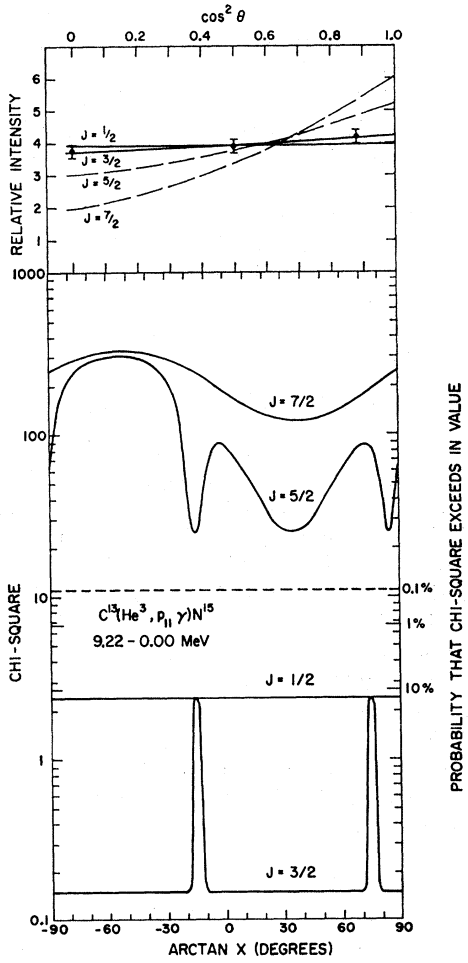

FIG. 18. Plot of χ^2 versus arctan x (the multipole mixing ratio) for the least-square analysis of the proton–γ-ray angular correlation measured for the ground-state decay of the 9.22-MeV level in N^{15} from the $C^{13}(He^3,p\gamma)N^{15}$ reaction. Values of $\frac{1}{2}$, $\frac{3}{2}$, $\frac{5}{2}$, and $\frac{7}{2}$ were assumed for the spin of the 9.22-MeV level. The best theoretical fits to the measured correlation for each value of the spin are also shown.

[45] A. H. Wapstra, G. J. Nijgh, and R. Van Lieshout, *Nuclear Spectroscopy Tables* (North-Holland Publishing Company, Amsterdam, 1959).

TABLE IV. Comparison of Legendre polynomial coefficients for the best theoretical and experimental fits to the angular-correlation measurements.

E_x (MeV)[a]	Experiment A_2/A_0	Experiment A_4/A_0	J	Theory A_2/A_0	Theory A_4/A_0
9.05	0.021±0.049	0.025±0.067	$\frac{3}{2}$	0.021	0
			$\frac{5}{2}$	0.377	0.116
			$\frac{7}{2}$	0.828	0.205
9.16	−0.307±0.036	−0.068±0.047	$\frac{3}{2}$	−0.318	0
			$\frac{5}{2}$	0.394	−0.111
			$\frac{7}{2}$	0.828	0.205
9.22	0.082±0.055	0.029±0.075	$\frac{3}{2}$	0.081	0
			$\frac{5}{2}$	0.379	0.098
			$\frac{7}{2}$	0.828	0.205

[a] All transitions $E_x \rightarrow$ ground state.

limits for which the probabilities of χ^2 exceeding their respective values is 10, 1, and 0.1%.[45] The expectation value of χ^2 is unity. If χ^2 for a possible value of the initial spin is nowhere less than the 0.1% limit, this value of the spin can for all practical purposes be eliminated. If the fit is nowhere less than the 1% limit, the assumed value of the spin can be ruled against with 99% certainty. At top of each figure the best fit (smallest χ^2) to the experimental measurements for each value of the initial spin is shown.

In Table IV the ratios A_2/A_0 and A_4/A_0 of the coefficients of the Legendre polynomials for the best theoretical fits obtained by the above method are compared to those determined by fitting the experimental data to the function

$$A_0+A_2P_2(\cos\theta_i)+A_4P_4(\cos\theta_i). \quad (4)$$

For our measurements at three angles θ_i, this expression gives a set of three simultaneous equations in three unknowns that can be solved exactly. For $J=\frac{1}{2}$, the theoretical coefficients A_2 and A_4 are identically zero. We see from Table IV and Figs. 16–18 that the correlation for the 9.05-MeV level is isotropic to within experimental error, so no choice can be made between the spins of $\frac{1}{2}$ and $\frac{3}{2}$. A spin of $\frac{3}{2}$ is the only possibility for the level at 9.16 MeV, although even here the best fit somewhat exceeds the expected value of unity for χ^2. The 9.22-MeV level probably has $J=\frac{3}{2}$; however $J=\frac{1}{2}$ is ruled against with only about 90% certainty. The multipole mixing ratio x is not determined by any of the measured correlations.

V. DISCUSSION

A. The 8.31-MeV Level

This level has been shown to have $J^\pi=\frac{1}{2}^+$ or $\frac{3}{2}^+$ from $N^{14}(d,p)N^{15}$ stripping measurements[19–21] and particle–γ-ray angular-correlation measurements.[24,25] This assignment is consistent with an electron-pair-correlation measurement[9] which showed that the multipolarity of the ground-state transition is $E1$. Because this level is is the only candidate below 9 MeV for the isobaric analog of the $\frac{1}{2}^+$ 7.55-MeV level[8,9] in O^{15}, a $\frac{1}{2}^+$ assignment is preferred. The agreement of the experimental branching ratios with those calculated for the second theoretical $\frac{1}{2}^+$ level of Halbert and French (see Table III) provides further evidence for identifying the spin and parity of the 8.31-MeV level as $\frac{1}{2}^+$.

B. The 8.57-MeV Level

$N^{14}(d,p)N^{15}$ stripping measurements[19,21] to this level favor a mixture of $l_n=0$ and $l_n=2$. A spin of $\frac{1}{2}$ is ruled out by γ-ray angular-correlation measurements and thus $J^\pi=\frac{3}{2}^+$ is implied.[25,26] Pair-correlation measurements confirm this assignment,[9] and it is further substantiated by the good agreement of the experimental and theoretical branching ratios (see Table III). The isobaric analog of this level has been identified[8,9] as the $\frac{3}{2}^+$ 8.28-MeV level in O^{15}.

C. The 9.05-MeV Level

Stripping measurements[19] favor $l_n=0$ and thus $J^\pi=\frac{1}{2}^+$ or $\frac{3}{2}^+$ for this level. Particle–γ-ray angular correlations (Table IV and Ref. 26) give an isotropic distribution, implying either $J=\frac{1}{2}$ or $\frac{3}{2}$, and pair-correlation measurements show that the ground-state transition is $E1$, requiring even parity.[9] A measurement[46] of the log ft value for the β decay of C^{15} to this level also indicates that $J^\pi=\frac{1}{2}^+$ or $\frac{3}{2}^+$. Because this level is the best candidate for the isobaric analog of the $\frac{1}{2}^+$ 8.75-MeV level in O^{15}, and because the experimental branching ratios are in good agreement with the third $\frac{1}{2}^+$ theoretical level of Halbert and French (see Table III), $J^\pi=\frac{1}{2}^+$ is preferred for the 9.05-MeV level.

D. The 9.16- and 9.22-MeV Levels

These levels are probably the isobaric analogs of the $\frac{3}{2}^+$ and $\frac{3}{2}^-$ levels in O^{15} at 8.915 and 8.980 MeV, respectively.[8,9] Particle–γ-ray angular-correlation measurements (Sec. IV) imply $J=\frac{3}{2}$ for both levels although there is a 10% probability of $J=\frac{1}{2}$ for the 9.22-MeV level. Pair-correlation measurements[9] imply odd parity for at least one of the levels, but it is not clear which one because they were unresolved in the measurements. The isobaric analogs of these levels are tentatively identified as indicated in Fig. 1 by comparing γ-ray branching ratios (Table II and Ref. 8).

The present branching ratios given in Table II for the 9.16-MeV level are the mean values of two measurements taken at incident energies of 2 and 5 MeV. The branching ratios for each measurement and for two previous measurements are given in Table V. Discrepancies between the measurements at 2 and 5 MeV in the present experiment are within possible uncertainties due to unknown angular-correlation effects.

[46] D. E. Alburger and K. W. Jones, Phys. Rev. **149**, 743 (1966).

There is some disagreement between the present measurements and previous $C^{13}(He^3,p\gamma)N^{15}$ branching ratios reported by Warburton *et al.*[9] for the 9.16-MeV level. This disagreement can be partially explained by the fact that in the previous measurements the 9.16-MeV level was incompletely resolved from the 9.22-MeV level. In the previous report the coincidence spectrum (Fig. 9 of Ref. 9) contains transitions from the 9.22-MeV state as well as the 9.16-MeV state. However, the apparent intensity of the peak labeled 2.83±0.02 MeV coupled with the absence of a 2.90-MeV peak with an intensity comparable to the 3.92-MeV peak is inconsistent with the present measurements (compare with Figs. 9 and 8) and is unexplained.

Both the present and previous $C^{13}(He^3,p\gamma)N^{15}$ measurements still disagree strongly with the $N^{14}(n,\gamma)N^{15}$ results. This has led Warburton and Olness[26] to suggest the possibility of a close-lying doublet with one level populated predominantly in the $C^{13}(He^3,p\gamma)N^{15}$ reaction and the other member of the doublet populated predominately in the $N^{14}(n,\gamma)N^{15}$ reaction. This possibility could also explain the fact that the best χ^2 fit to the angular correlation for this level, for $J=\frac{3}{2}$, achieves only about a 20% probability (Fig. 17). Correspondingly, a small P_4 term appears necessary to fit the experimental data by a series of even Legendre polynomials (Table IV); however, P_4 cannot occur in the theoretical distribution for $J=\frac{3}{2}$. It should also be noted that the previous $C^{13}(He^3,p\gamma)N^{15}$ measurements[9] were taken at an incident He^3 energy (3 MeV) different from either of the present measurements. The two levels of the suggested doublet could be populated in significantly different proportions at different incident energies in the same reaction. This provides another possible explanation for the discrepancy between the present results and those reported previously for the $C^{13}(He^3,p\gamma)N^{15}$ reaction. However, in recent magnetic-spectrograph measurements,[14] no evidence was found for a 9.16-MeV doublet separated in energy by more than 8 keV. Thus, further investigation of the 9.16- and 9.22-MeV levels is needed. Because a $N^{14}(d,p)N^{15}$ stripping measurement could determine the parities of these levels, and branching-ratio measurements from other reactions such as $N^{14}(d,p\gamma)N^{15}$ would shed light on the question of a close-lying doublet at 9.16 MeV, this reaction has been investigated in this laboratory.[47] Branching-ratio measurements for the 9.16 "state" using the $N^{14}(d,p\gamma)N^{15}$ reaction are in good agreement with the results of Warburton *et al.*[9] and in disagreement with the present results using the $C^{13}(He^3,p\gamma)N^{15}$ reaction. These results indicate that both members of the suggested doublet are populated with comparable intensities in the $N^{14}(d,p)N^{15}$ reaction. A report of this work will be presented elsewhere.

TABLE V. Comparison of experimental branching ratios of the 9.16-MeV level in N^{15}.

E_f (MeV)	E_γ (MeV) \ E_{He^3}	Present data $C^{13}(He^3,p\gamma)N^{15}$ 2 MeV (%)	5 MeV (%)	Warburton *et al.*[a] $C^{13}(He^3,p\gamma)N^{15}$ 3 MeV (%)	Carter and Motz[b] $N^{14}(n,\gamma)N^{15}$ (%)
0	9.16	88.9±1.1	80.5±1.6	56±10	18
5.27	3.89 }	3.9±0.5	7.3±0.8	7±3	10 (to 5.27)
5.30	3.86 }				
6.32	2.84	2.0±0.4	3.7±0.6	10±5	20
7.15	2.01	5.2±0.7	8.5±1.2	23±5	52
7.30	7.30[c]	<2	<2	4±2	...
7.56	1.60	<1	<1	<5	...
8.31	0.85	...	<1	<0.5	...

[a] Reference 9.
[b] References 27 and 28.
[c] Decay to E_f not observed, branching ratio obtained from cascade γ ray listed.

E. The 9.76- and 9.83-MeV Levels

Proton–γ-ray angular-correlation measurements[26] imply $J=\frac{5}{2}$ for the 9.76-MeV level. Pair-correlation measurements[9] on the ground-state decay favor $E1$, but uncertainties were large enough to admit an $E2$ transition. Only $J^\pi=\frac{5}{2}^-$ is consistent with these two measurements.[26] The branching ratios are also consistent with $J=\frac{5}{2}$ (implied by the relative strength of the transition to the $\frac{7}{2}^+$ level at 7.56 MeV) and odd parity (implied by the predominance of the ground-state decay and the relative weakness of the decay to the $\frac{3}{2}^-$ level at 6.32 MeV). The isobaric analog of this level has been identified[10] as the $\frac{5}{2}^{(-)}$ 9.49-MeV level in O^{15}.

The 9.83-MeV level has no observable ground-state transition (Fig. 11 and Table II). Proton–γ-ray angular-correlation measurements[26] for the cascade through the 5.27-MeV level require $J=\frac{7}{2}$ for the 9.83-MeV level This is consistent with the absence of an observable ground-state transition and the predominance of the decay to the $\frac{5}{2}^+$ level at 5.27 MeV (84%). The fact that a decay to the $\frac{3}{2}^-$ level at 6.32 MeV is observed makes an $E2$ assignment for the transition preferable. This implies odd parity for the 9.83-MeV level, but further confirmatory evidence for this assignment is desirable.

F. The 9.93- and 10.07-MeV Levels

These are the last two bound levels in N^{15}. The ground-state transition for the 9.93-MeV level has an isotropic angular correlation[26] implying $J=\frac{1}{2}$ or $\frac{3}{2}$. Pair-correlation measurements[9] imply $E1$ for the ground-state transition and thus $J^\pi=\frac{1}{2}^+$ or $\frac{3}{2}^+$. Either of these is consistent with the observed branching ratios.

From angular-correlation measurements[26] the 10.07-MeV level has $J=\frac{3}{2}$. Pair-correlation measurements[9] imply an $E1$ ground-state transition. The strength of this transition and the relative weakness of the only other observed decay, to the 5.3-MeV doublet (Table II), is consistent with an assignment of $\frac{3}{2}^+$ for the 10.07-MeV level.

[47] F. C. Young and C. Steerman (private communication).

G. The 10.45-MeV Level

Angular-correlation measurements[26] are inconclusive for this level. $J<\frac{5}{2}$ is unlikely from the decay scheme, and $J>\frac{7}{2}$ can be ruled out by the lifetime limit derived from the measured γ-ray partial width.[26] If this state were $\frac{5}{2}^-$, one would expect to observe a ground-state transition (compare with the 9.76-MeV level). If this state were $\frac{7}{2}^+$, one would not expect to observe a strong branch to the $\frac{3}{2}^-$ level at 6.32 MeV (via $M2$ or $E3$). The absence of an observable ground-state transition ($<4\%$) and the relative strength (15%) of the decay to the 6.32-MeV level makes $J^\pi=\frac{5}{2}^+$ or $\frac{7}{2}^-$ preferable.

VI. CONCLUSIONS

Nine experimental levels in N^{15} below 9 MeV have been identified with their isobaric-analog levels in O^{15} and with theoretical shell-model levels of Kurath[2] and Halbert and French.[3,4] There is some crossing of levels between N^{15} and O^{15}, perhaps due to Coulomb effects. For the levels above 9 MeV in N^{15} it is apparent that higher-order shell-model configurations are significant, and further theoretical work is necessary. It seems likely that the triplet of levels at 9.05, 9.16, and 9.22 MeV in N^{15} includes the analogs of the $\frac{1}{2}^+$, $\frac{3}{2}^{(+)}$, and $\frac{3}{2}^-$ levels at 8.24, 8.92, and 8.98 MeV, respectively, in O^{15}, although the ordering of the levels in N^{15} is still uncertain. For the higher-energy levels, more information is needed on the spins and parities of possible analog levels in O^{15}.

These results constitute an impressive success of the shell-model for $A=15$. There is surprisingly good agreement between experimental and theoretical branching ratios for the 8.31-, 8.57-, and 9.05-MeV levels in N^{15}. Some caution is necessary here, however, because of the complete dissimilarity between the decay schemes for the 8.31-MeV level in N^{15}, with a 79% ground-state branch (Table II), and its apparent analog at 7.55 MeV in O^{15}, which decays predominately (57%) to the $\frac{3}{2}^-$ level at 6.18 MeV with only a 3% branch to the ground state.[9] It has been suggested[9] that a small change in the wave function, due to Coulomb effects and the proximity of the $N^{14}+p$ threshold at 7.29 MeV in O^{15}, could greatly affect the transition strengths because of possible cancellations in the matrix elements (see also Ref. 48). It is certainly unreasonable to expect the expansion of Halbert and French in terms of wave functions for an infinite harmonic-oscillator potential to give a complete description of the levels in O^{15} above the threshold for particle emission, where the finite depth of the nuclear potential becomes of primary importance. However, in N^{15} the levels for which comparison was made between theoretical and experimental branching ratios are well below the $C^{14}+p$ threshold at 10.21 MeV so that all particles are tightly bound in the potential well, and the good agreement of the experimental results with theory is therefore considered significant.

[48] E. K. Warburton, in *Isobaric Spin in Nuclear Physics*, edited by J. D. Fox and D. Robson (Academic Press Inc., New York, 1966), p. 90.

ACKNOWLEDGMENT

Computational support by the National Aeronautics and Space Administration Research Grant No. NsG-398 to the Computer Science Center of the University of Maryland is gratefully acknowledged.

APPENDIX: ANALYSIS OF ERRORS IN BRANCHING RATIOS

Consider a level which decays by branches i with measured strengths $n_i\pm\sigma_{n_i}$ so that the total strength is $N=\sum_i n_i$. The branching ratios are defined by $\alpha_i\equiv n_i/N$ so that $\sum_i \alpha_i=1$. The percent error in α_i is not simply the percent error in n_i, since for a strong branch n_i the total strength N depends strongly on n_i. The standard deviations σ_{n_i} and $\sigma_N=(\sum_i \sigma_{n_i}{}^2)^{1/2}$ are not independent. To circumvent this difficulty, define an independent quantity $\bar{N}_i$ by

$$\bar{N}_i\equiv\sum_{j\neq i} n_j=N-n_i.$$

Then the error

$$\sigma_{\bar{N}_i}=(\sum_{j\neq i} \sigma_{n_j}{}^2)^{1/2}$$

is independent of σ_{n_i}. The branching ratio can be expressed as $\alpha_i=n_i/(n_i+\bar{N}_i)$. The error in α_i is found by taking the variation of α_i with respect to n_i and $\bar{N}_i$:

$$\delta\alpha_i=\frac{N-n_i}{N^2}\delta n_i-\frac{n_i}{N^2}\delta\bar{N}_i.$$

The standard deviation in the branching ratio then becomes

$$\sigma_{\alpha_i}{}^2=\left(\frac{N-n_i}{N^2}\sigma_{n_i}\right)^2+\left(\frac{n_i}{N^2}\sigma_{\bar{N}_i}\right)^2.$$

Note that for weak branches the first term predominates, but for strong branches the second term predominates. For example, for the 9.05-MeV ground-state decay, the error in the strength is 6%, but the error in the branching ratio is only 1%. Finally, if there are only two branches (as for the 10.07-MeV state), the errors for each branch are identical. Of course, unobserved branches are neglected in this analysis.